Tracking the volatile and magmatic history of Vesta from chromium stable isotope variations in eucrite and diogenite meteorites

Ke Zhu, Paolo Sossi, Julien Siebert, Frédéric Moynier

Tracking the volatile and magmatic history of Vesta from chromium stable isotope variations in eucrite and diogenite meteorites

Ke Zhu (朱柯)[1*], Paolo A. Sossi[1], Julien Siebert[1], Frédéric Moynier[1,2]

[1]Institut de Physique du Globe de Paris, Université de Paris, CNRS, 1 rue Jussieu, Paris 75005, France

[2]Institut Universitaire de France, Paris, France

*corresponding author: zhu@ipgp.fr

Key words: Cr isotopes, Vesta, chondrites, volatile elements, volatile history, equilibrium fractionation, howardite-eucrite-diogenite, magma ocean

Resubmitted to GCA on July 24th, 2019

Abstract

Although Solar System bodies exhibit large variations in their volatile element abundances, the mechanisms and conditions that lead to these variations remain ambiguous. The howardite-eucrite-diogenite (HED) meteorites that likely sample the asteroid 4 Vesta, provide evidence for extensive volatile depletion on their parent body. Isotopic variations in moderately volatile elements, such as Zn, have been used to track the origin of such volatile loss. Although not nominally volatile, Cr is useful because it has several oxidized gas species that render it volatile under the oxidizing conditions that characterize planetary accretion. As such, volatile loss of Cr has the potential to produce an isotopically light evaporation residue under an equilibrium regime. This contrasts with other moderately volatile elements that show heavy isotope enrichments in the residue following both kinetic or equilibrium fractionation. Here, we report the Cr stable isotope composition of 11 eucrites and four diogenites. The eucrites possess systematically lighter Cr isotope compositions than diogenites, which is onset by the accumulation of isotopically heavy Cr^{3+}-rich orthopyroxene and spinel in diogenites during their magmatic evolution. We estimate for the primary eucrite melt with Mg# ≈ 50, a $\delta^{53}Cr$ ($^{53}Cr/^{52}Cr$ deviation relative to NIST SRM 979 in per mile) of -0.22 ± 0.03 ‰ (2SD), lighter than any chondritic meteorite group by ~0.1 ‰. This deficit may result from either partial melting with residual Cr^{3+}-bearing phases (e.g. chromite) that retain heavy isotopes, or from vapor loss that occurred at equilibrium with a magma ocean on Vesta. Isotopic fractionation during partial melting would necessitate implausibly high Cr contents in the Vestan mantle, and oxygen fugacities high enough to stabilize

chromite in the mantle source. Isotopic fractionation during evaporation would require an oxidized vapor and a reduced residue, as predicted by thermodynamic constraints on the composition of the vapor phase above a silicate magma ocean. Therefore, this Cr isotopic deficit between Vesta and chondrites may be caused by Cr loss at relatively high oxygen fugacity in a gas phase at equilibrium with the liquid from which it evolved. Temperatures of volatile loss are estimated to be lower than 2300 K, consistent with loss from a large-scale magma ocean model for formation of Vesta, which may be a common evolutionary stage in accreting planetesimals.

1. Introduction

Differentiated planetary bodies are characterized by a widespread depletion in their moderately volatile element abundances (e.g. O'Neill and Palme, 2008). The mechanisms and timing of this moderately volatile element depletion observed in the silicate fraction of differentiated bodies is still debated (e.g. O'Neill and Palme 2008; Hans et al., 2013; Day and Moynier, 2014; Siebert et al., 2018; Sossi and Fegley 2018)

Recent measurements of the stable isotope compositions of moderately volatile elements (such as Zn, Cl, Ga, K, Rb) in planetary materials have provided new insights into the origin, and conditions of the volatile depletion in Solar System materials (Sharp et al., 2010; Paniello et al., 2012a; Kato et al., 2015; Wang and Jacobsen, 2016; Kato and Moynier, 2017; Pringle and Moynier, 2017; Boyce et al. 2018). These studies have found that, in general, moderately volatile elements were enriched in their heavier isotopes in volatile depleted bodies such as 4 Vesta (e.g. Paniello et al., 2012b; Pringle

64 and Moynier, 2017; Sarafian et al., 2017; Tian et al., 2018) relative to their putative
65 chondritic building-blocks. These results point toward evaporation during planetary
66 processes such as impacts (e.g. Paniello et al., 2012a; Wang and Jacobsen, 2016),
67 degassing during eruption (Sharp et al., 2010) or crystallization of a magma ocean (e.g.
68 Day and Moynier, 2014; Boyce et al., 2015; Kato et al., 2015; Kato and Moynier, 2017)
69 that are absent during chondrite formation.

70 Based on spectroscopic data, the howardite-eucrite-diogenite (HED) clan of
71 meteorites are interpreted as samples of the crust of 4 Vesta, the second largest asteroid
72 in the asteroid belt (McCord et al., 1970; Binzel and Xu, 1993; Beck et al. 2011; Russell
73 et al., 2012). Eucrites are broadly basaltic rocks predominantly composed of pigeonite
74 and plagioclase, derived from Vesta's crust, whereas diogenites are mostly
75 orthopyroxenites, with some olivine-rich variants, and are conventionally viewed as
76 cumulate igneous rocks formed in a magma ocean or during intrusive magmatism on
77 Vesta; howardites are impact-brecciated mixtures of both (Mittlefehldt, 2015).

78 Howardite-eucrite-diogenite meteorites (HEDs) are highly depleted in moderately
79 volatile elements as illustrated by K/U and Rb/Sr ratios ~10 times, and ~100 times lower
80 than in CI chondrites, respectively (Day and Moynier, 2014; Mittlefehldt, 2014). There
81 is limited data available on the stable isotope composition of moderately volatile
82 elements in HEDs, e.g. Zn, Rb, Cl and Li (Magna et al., 2014; Paniello et al., 2012b;
83 Pringle and Moynier, 2017; Sarafian et al., 2017). Zinc and Rb with 50%-nebular
84 condensation temperatures (T_c) of 726 K and 800 K, respectively (Lodders 2003) are

85 enriched in the heavier isotopes in HED meteorites compared to chondrites (Paniello et
86 al., 2012b; Pringle and Moynier, 2017). Chlorine (T_c = 948 K, Lodders 2003) isotope
87 ratios correlate with major- (e. g. Mg and Cr) and trace-element (K, Sc and Br) content,
88 which suggests mineral (e. g. olivines and spinel) crystallization and volatile loss (e. g.
89 K and Br) during a magma ocean stage (Sarafian et al., 2017). All of the three isotope
90 systems above point toward volatile depletion due to evaporation from 4 Vesta (Paniello
91 et al., 2012b; Pringle and Moynier, 2017; Sarafian et al., 2017). On the other hand, Li
92 with a T_c of 1142 K, is isotopically similar to chondrites (Magna et al., 2014). The
93 absence of Li isotopic fractionation and limited Li loss would suggest that the
94 temperature under which this occurred was relatively low (Magna et al., 2014). Based
95 on Rb-Sr isotope dating, Hans et al. (2013) suggested that volatile loss occurred under
96 solar nebula conditions, while others have argued for post-nebular loss under more
97 oxidizing conditions (O'Neill and Palme, 2008; Moynier et al., 2012). Since both Zn
98 and Rb have more reduced species (Zn^0 and Rb^0) in the vapor compared to silicate melts
99 (Zn^{2+} and Rb^+) (Lamoreaux and Hildenbrand, 1984; Lamoreaux et al., 1987; Sossi et
100 al. 2019), both equilibrium and kinetic evaporation would enrich these elements in the
101 heavier isotopes in the condensed phase(s), because the vapor (compared to residue)
102 and reduced species (compared to oxidized species) are both enriched in the lighter
103 isotope. It is therefore not presently possible to discern between these two kinds of
104 isotopic fractionation processes based on these isotopic systems. As recently applied by
105 Sossi et al. (2018), Cr isotopes can be used to give insights into the mechanism of
106 volatile depletion. Under oxidizing conditions (fO_2 > IW+1), relevant to planetary

evaporation (Visscher and Fegley, 2013), Cr may be present in the gas as oxide species CrO(g), CrO_2(g) and CrO_3(g) (Chase, 1998) and equilibrium isotopic fractionation (Young et al., 2019) could cause enrichment of the lighter isotopes in the condensed phases, in which Cr is either di- or trivalent, relative to the vapor. This contrasts with its speciation under nebular conditions, in which Cr may be present as Cr^{2+} or Cr metal in the condensed phase and Cr^0 in the gas. Sossi et al. (2018) have shown that the Moon is enriched in the lighter isotopes of Cr compared to Earth's mantle, its likely precursor, a feature ascribed to volatile loss under relatively oxidizing conditions, which cause Cr to be present as CrO_2 in the vapor phase but predominantly as Cr^{2+} in the melt. Because this signature could only have resulted from equilibrium between liquid and gas, they were able to calculate that evaporation must have occurred at temperatures between 1600 and 1800 K, implying that loss took place following cooling and accretion of the Moon. This contrasts with models that argue for volatile loss contemporaneous with a very hot (>4000 K) giant impact (Nakajima and Stevenson, 2014). Moreover, relative to other moderately volatile elements such as Zn or K (whose abundances in lunar basalts are ~50 (K) to ~300 (Zn) times lower than those in chondrites; Paniello et al., 2012; Day and Moynier, 2014), the i) higher concentration of Cr (Wänke and Dreibus, 1980) and ii) its lower volatility (Sossi et al., 2018) facilitate precise isotopic analysis and make Cr less susceptible to overprinting by possible late accretion on Vesta.

Previous studies show that Cr isotopes do not fractionate during core-mantle differentiation, as evidenced by experimental studies (Bonnand et al., 2016b) and the homogeneous Cr isotope composition of chondrites and estimates for the bulk silicate

Earth (Bonnand et al., 2016b; Schoenberg et al., 2016; Sossi et al., 2018). Moreover, Cr is not appreciably siderophile (*e.g.,* Rammensee et al. 1983) except under very high temperatures and/or reducing conditions (Wade and Wood, 2001; Mann et al. 2009; Siebert et al. 2013). Therefore, isotopic variations in Cr likely reflect other processes, such as magmatic differentiation and/or volatile depletion instead of core formation. Studying the Cr isotopic composition of HED meteorites may be used to evaluate the redox conditions during volatile loss of the HEDs and to estimate whether the volatilization occurred during equilibrium or kinetic conditions, thereby potentially constraining the temperature of evaporation. While there are no systematic studies of the Cr isotope composition of eucrites and diogenites, the scarce data suggest a hint of a light isotope enrichment in eucrites compared to diogenites and chondrites (Qin et al., 2015; Bonnand et al., 2016b). Here, we report high-precision Cr isotope compositions of 11 eucrites and four diogenites analyzed via double-spike technique by Multi-Collector Inductively-Coupled Plasma Mass Spectrometer (MC-ICP-MS) to better quantify the magmatic and evaporation/condensation process that occurred during Vesta's formation and constrain its physicochemical conditions.

2. Samples and analytical methods

2.1 Samples

Eleven eucrites and four diogenites were studied. The eucrites comprise Pasamonte, Camel Donga, Stannern, Bouvante, Jonzac, Juvinas, EET 87548, Moore County, Pomozdino, Serra de Magé and EET 87542, and the diogenites include EET

79002, Tatahouine, LAP 03569 and Shalka. Two different groups of eucrites, Main group and Stannern trend (including Stannern, Pomozdino and Bouvante), have been studied. The Stannern trend eucrites (on basis of their Mg# (molar Mg/(Mg+Fe), Ti and incompatible trace element abundances) may be contaminated by Vestan crustal materials (Barrat et al., 2007). Pasamonte was recognized as an anomalous eucrite based on a different O isotopic composition compared to most HEDs (Greenwood et al., 2009), suggesting that it may not have originated from Vesta or that Vesta is isotopically heterogeneous. Most of the eucrites selected are monomict breccias, and the sample descriptions are summarized in Table 1. Full replicates, including dissolution, spike addition, and chemical purification of Pasamonte, Juvinas and Jonzac were performed in order to test the overall reproducibility of the method. The Cr isotopic composition of three terrestrial geological reference materials, BHVO-2 and DTS-1 and PCC-1 were analyzed to quantify the accuracy of the method.

2.2 Methods

All sample processing was performed in the clean laboratory at the Institut de Physical du Globe de Paris (IPGP) following the method described in Sossi et al., (2018). Ten to 20 mg of each meteorite sample were weighed from original powder of ~1g to ensure homogeneity. All eucrites were firstly dissolved in a mixture of HF and HNO_3 (2:1) on a hot plate (130 °C) for two days. Subsequently, the samples were dissolved in aqua regia (concentrated HCl and HNO_3 mixture in 3:1 ratio) to ensure complete digestion. The four diogenites were dissolved by the concentrated mixed acid

(HCl: HF: HNO_3 = 5:3:2) in Parr Bombs under pressurized steel jackets for four days at 180 °C, and no visible residues were observed. Then, the adequate amount of ^{50}Cr-^{54}Cr double spike (28% of the Cr content endemic to the sample) was added and the solution and refluxed in closed PFA beakers at 120 °C overnight. Half of the digested samples were chemically purified for Cr via a two-step cation exchange chromatography adapted from Trinquier et al. (2008), as routinely undertaken at IPGP (Mougel et al., 2017; Mougel et al., 2018). This method has a total procedural yield of 60~90% and blank of ~5 ng of Cr. Compared to the total 10-60 μg of Cr, the blank is negligible. The final Cr cut was evaporated in concentrated HNO_3 drops three to five times to convert the HCl medium to HNO_3, and to remove leftover organics (i.e. resin), and then diluted to a concentration of 1 ppm Cr, in 2% (0.317 M) HNO_3 for isotope analysis.

The Cr stable isotope compositions of these purified samples were measured on a Thermo Scientific Neptune Plus MC-ICP-MS housed at the IPGP, the details are described in Sossi et al. (2018). The isotopic ratio for samples is compared to NIST SRM 979 and reported in delta notation:

$$\delta^{53}Cr(‰) = \left(\frac{\left(^{53}Cr/^{52}Cr\right)_{sample}}{\left(^{53}Cr/^{52}Cr\right)_{NIST\ SRM\ 979}} - 1\right) \times 1000. \quad (1)$$

The Cr isotopic composition of a secondary standard, NIST SRM 3112a, was also measured in each analytical session to monitor the instrumental mass fractionation and the precision of the data. The Cr isotopic composition of every sample was measured

191 twice. Therefore, the Cr isotopic composition of samples for which 2 separate chemical
192 purification procedures were performed (Stannern, Pasamonte, Juvinas and Jonzac)
193 were analyzed four times (in figures, two replicate data for the four samples were
194 combined as one). The uncertainties quoted for individual samples are 2SD of single
195 sample measurements (100 cycles for two times) or 2SD reproducibility of several
196 NIST SRM 979 measurements in the same analytical session (0.04‰), or that of NIST
197 SRM 3112a (0.04‰), whichever is largest.

198 Since, when normalized to the $^{50}Cr/^{52}Cr$ ratio, Cr shows non-mass dependent
199 isotopic effects on both the $^{53}Cr/^{52}Cr$ (due to the decay of ^{53}Mn) and on $^{54}Cr/^{52}Cr$
200 (nucleosynthetic anomalies) ratios in HEDs (Trinquier et al., 2007), a correction must
201 be applied in order to properly perform the double spike reduction. Most samples
202 analyzed here had been previously studied for their ^{53}Cr and ^{54}Cr anomalies. For the
203 samples (Camel Donga, EET 87548, Moore County, Pomozdino, Serra de Magé, EET
204 87542 and EET 79002), which have no available data, we have used the average of the
205 ^{54}Cr anomalies which have been shown to be homogeneous between all HED analyzed,
206 with an average value for $\varepsilon^{54}Cr$ of -0.74. Since ^{53}Cr is produced by the radioactive decay
207 of ^{53}Mn (e.g. Zhu et al., 2019a; Zhu et al., 2019b), one single value cannot be applied
208 and for the samples for which the ^{53}Cr anomalies were not available and the ^{53}Cr
209 anomalies were estimated based on their $^{55}Mn/^{52}Cr$ ratio and from the slope of the ^{53}Mn-
210 ^{53}Cr isochron (Trinquier et al., 2008).

211 Pasamonte is anomalous and has heterogeneous O and Cr isotope compositions

(Scott et al., 2009; Sanborn and Yin, 2014). Sanborn and Yin (2014) reported $\varepsilon^{54}Cr$ = -0.33 ± 0.08, while Trinquier et al. (2007) reported -0.71 ± 0.08 on a different sample section. However, it should be noted that whichever $\varepsilon^{54}Cr$ values applied in the double spike reduction only changes the calculated $\delta^{53}Cr$ by 0.02, which is smaller than the 2SD error for NIST SRM 979. Furthermore, if the variation for $\varepsilon^{53}Cr$ or $\varepsilon^{54}Cr$ reaches 1ε (the variation for $\varepsilon^{53}Cr$ and $\varepsilon^{54}Cr$ in HEDs is always less than 0.6ε (Sanborn and Yin, 2014; Trinquier et al., 2007; 2008) and were not corrected, the final corrected $\delta^{53}Cr$ would only shift by 0.008‰ due to $\varepsilon^{53}Cr$ and 0.038‰ due to $\varepsilon^{54}Cr$ which would fall within the analytical uncertainty (0.04‰). For consistency, we use only the $\varepsilon^{54}Cr$ data from Trinquier et al. (2007) for the samples for which $\varepsilon^{54}Cr$ is unknown.

3 Results

The $\delta^{53}Cr$ values, Cr contents and Mg# of 11 eucrites (including seven non-cumulate eucrites, three cumulate eucrites and one polymict eucrite) and five diogenites (including one datum, from Bonnand et al. (2016b)) are reported in the Table 1. The $\delta^{53}Cr$ for eucrite samples ranges from -0.13 to -0.25 ‰, with an average value of -0.20 ± 0.08 ‰ (2SD, n=11), twice as large as the analytical uncertainty. Compared to cumulate eucrites, the non-cumulate eucrites are characterized by lower Cr content, lower Mg# and lower $\delta^{53}Cr$ than the diogenites. The five diogenite samples display heavier $\delta^{53}Cr$, with the LAP 03569 sample having the heaviest $\delta^{53}Cr$ values of -0.07 ± 0.04 ‰. There is no systematic difference in the Cr isotope composition between the main group and Stannern trend eucrites when comparing the five monomict eucrites:

Juvinas, Jonzac, Camel Donga, Stannern and Bouvante. Replicate analyses of the $\delta^{53}Cr$ of Pasamonte, Juvinas, Jonzac and Stannern agree within error (see table 1). The $\delta^{53}Cr$ of the USGS standards, BHVO-2, PCC-1 and DTS-1, are consistent with previously reported values (Schoenberg et al., 2016; Sossi et al., 2018; Chen et al., 2019). When $\delta^{53}Cr$ values are reported as a function of Cr concentration (and Mg#), diogenites and eucrites are clustered, with eucrites isotopically light and low in Cr (1750 ~ 5673 ppm) compared to the isotopically heavier and Cr-richer diogenites (4404 ~ 6780 ppm) (Figure 1a). The Mg# of the HED meteorites analyzed are also grouped into a high (Mg# ≈ 75, diogenites) and a low (Mg# ≈ 40, basaltic eucrites) populations, with some cumulate and magnesian eucrites spanning the gap between them (Figure 1b).

4. Discussion

4.1 Heavy Cr isotope enrichment in diogenites

Eucrites and diogenites are samples from the silicate fraction of Vesta (Keil, 2002; Mittlefehldt, 2015). The isotopically heavier diogenites have higher Cr contents and Mg# relative to eucrites. This suggests that magmatic differentiation could have led to the Cr isotopic difference between the two meteorite groups. Small variations on the order of 0.1 ~ 0.2 ‰ are also found in lunar mare basalts and Mg suite cumulates (Bonnand et al., 2016a; Sossi et al., 2018). Fractionation is generally more limited in Earth's mantle (-0.11 ± 0.06 ‰; Schoenberg et al., 2008; Sossi et al., 2018), except during metasomatic processes (Xia et al., 2017; Shen et al., 2018). Therefore, utilizing the eucrites and diogenites to reconstruct the Cr isotopic composition of Vesta requires

assessment of any isotopic fractionation that may have occurred during processes such as partial melting and fractional crystallization.

Partial melting on Earth involves isotopic exchange between both Cr^{2+}- and Cr^{3+}-bearing phases. In typical mantle peridotites that have equilibrated near the Fayalite-Magnetite-Quartz (FMQ) buffer, the majority of Cr is present in its trivalent form in spinel and clinopyroxene (Li et al., 1995). At the same fO_2, basaltic melts have a greater proportion of Cr^{2+}, about $Cr^{2+}/\sum Cr = 0.3$ at 1400°C (Berry et al., 2006). The difference in Cr redox states (Cr^{2+} and Cr^{3+}) between residual mantle and melt thereby provides a mechanism for inducing Cr isotope fractionation (the heavier Cr^{3+} is highly compatible in some refractory minerals; e.g. chromite), in which the residue becomes isotopically heavier and the complementary liquids are relatively lighter. Shen et al. (2018) calculated the magnitude of this effect, and found a $\Delta^{53}Cr_{Mantle\text{-}Melt} = +0.05$ ‰ for degrees of melting around 15% (i.e., melts should be isotopically lighter than their sources). Nevertheless, observational evidence points to limited Cr isotope fractionation during partial melting near the FMQ buffer (Schoenberg et al., 2008) on the basis that both terrestrial basaltic rocks and peridotites have similar compositions.

On Vesta, basaltic eucrites have assemblages that reflect equilibration at lower fO_2 relative to terrestrial magmas, ≈1 log unit below the Iron-Wüstite buffer (e.g. Righter et al., 2016) yielding $Cr^{2+}/\sum Cr \approx 0.9$ in the melt using the calibration of Berry et al. (2006). Mineral phases in equilibrium with eucritic liquids (pyroxene-plagioclase ± spinel ± metal; Bartels and Grove, 1991; Stolper, 1977) have the majority of their Cr

hosted in pyroxene and spinel. Even at IW-1, these phases will contain predominantly Cr^{3+} (Karner et al., 2007). Should these minerals be present as residual phases during partial melting to produce eucrites, then the large $Cr^{2+}/\sum Cr_{melt} > Cr^{2+}/\sum Cr_{source}$ should enhance fractionation relative to terrestrial environments. The $Cr^{2+}/\sum Cr_{source}$ of the Vestan mantle source will depend on the phase assemblage. A peridotitic source at IW-1 and 1400 °C, would contain olivine with $Cr^{2+}/\sum Cr \approx 0.8$ to 0.9 (Bell et al. 2014), low-Ca clinopyroxene with exclusively Cr^{3+} (Karner et al. 2007), with orthopyroxene between these two extremes, conferring a weighted average ≈ 0.5. The net effect is to produce isotopically light partial melts, unless i) spinel is not stable at partial melting temperatures (Li et al., 1995) or ii) spinel and much of the pyroxene is completely dissolved from eucrite parent magma source regions. If the Cr content of the Vestan mantle is ≈ 2300 ppm (see Jones (1984) and discussion below) and given that D_{Cr} between mantle and melt is approximately unity (Hanson and Jones, 1984; Mallmann and O'Neill, 2009), then the relatively high Cr content of main group eucrites (≈ 2000 ppm which mainly resides in spinel and pyroxene; Barrat et al., 2000) compared to terrestrial basalts (≈ 300 ppm) suggests it behaved as a moderately incompatible element during partial melting on Vesta, implying spinel was not an important residual phase. This is also borne out in the increasing Cr contents with progressive fractional crystallization among main group eucrites (see Barrat et al., 2000). Importantly, the melt phase thus leverages the Cr isotope composition of the system for eucrites, whereas the majority of the Cr remains in the mantle during partial melting on Earth. However, the effect of partial melting cannot be excluded, and would produce partial melts with

297 lighter Cr isotope compositions than their sources (Figure 2).

298 To interpret the causes of Cr isotope variations in eucrites and diogenites requires
299 understanding of their petrogenesis. One prevailing hypothesis states that diogenites
300 and eucrites originated from an early Vestan magma ocean, and melts parental to
301 eucrites were formed followed by crystallization of cumulate pyroxenes, which would
302 imply that diogenites and eucrites were cogenetic (Mason, 1967; Righter and Drake,
303 1997; Mandler and Elkins-Tanton, 2013). However, the diversity in diogenite
304 compositions have been used as evidence to preclude a direct link to eucrites (Stolper,
305 1977; Barrat et al. 2008). Therefore, in order to determine the Cr isotope composition
306 of Vesta, the effects of fractional crystallization in fractionating Cr isotopes must first
307 be understood.

308 The majority of diogenites are coarse-grained ultramafic rocks dominated by
309 magnesian orthopyroxenes and minor olivine, silica and spinel (Bowman et al., 1997;
310 Beck and Mcsween, 2010), while eucrites are mainly comprised of orthopyroxene,
311 pigeonite, low-Ca pyroxenes, plagioclases and minor silica, ilmenite and spinel
312 (Delaney et al., 1984; Mittlefehldt, 2015). Among these minerals, pyroxene (both
313 orthopyroxenes and clinopyroxenes) and chromite are the main carrier phases for Cr,
314 and together account for more than 98% of the Cr budget in eucrites and diogenites, as
315 will be discussed below. In detail, the pyroxenes, which account for 40~60% in mass
316 of eucrites (including orthopyroxene, pigeonite and high-Ca pyroxene), contain an
317 average of 0.32 wt% Cr_2O_3, while plagioclase (~40% of eucrites) are mostly Cr-free

(Mayne et al., 2009). Despite spinel being a minor mineral in eucrites (0.3% in mode), it can contain ~45 wt% of Cr_2O_3, and is therefore an important Cr contributor to bulk eucrites. Ilmenite is another Cr-bearing mineral (~0.4 wt% of Cr), but its proportion in eucrites is only ~0.7% (Mittlefehldt, 2015), of which Cr contribution to bulk rock is less than 1%. Relative to eucrites, diogenites have different mineral modes and compositions. Most diogenites comprise 85~99% orthopyroxene, which have on average 0.41 wt% of Cr_2O_3, and 0.7% spinels that can hold up to 55 wt% of Cr_2O_3 in diogenites (Beck and McSween, 2010; Day et al., 2012). In both eucrites and diogenites, the ratio, $[Cr]_{pyroxene}$: $[Cr]_{spinel}$, is close to 1 : 1.

Chromite (Cr-spinel) hosts exclusively Cr^{3+} in octahedral coordination that confers a normal site distribution on spinel. Its formation from the melt can be described following Roeder and Reynolds (1991) as:

$$MgO(l) + 2CrO_{1.5}(l) = MgCr_2O_4(s). \quad (2)$$

The activity of $CrO_{1.5}$ in the melt is related to fO_2 by homogeneous equilibrium with CrO:

$$CrO(l) + ¼O_2 = CrO_{1.5}(l). \quad (3)$$

As reaction (3) is associated with a strongly negative change in entropy, $\Delta S^\circ_{(3)}$ (Li et al. 1995), the crystallization of Mg-rich, Cr-spinel is favoured at i) high fO_2 and ii) low temperatures. Trivalent Cr is also preferentially incorporated into pyroxene (Mallmann and O'Neill, 2009), that is to say, $Cr^{3+}/Cr^{2+}_{px,spinel} > Cr^{3+}/Cr^{2+}_{melt}$. Chromium

isotope fractionation occurs between the Cr^{2+}- and Cr^{3+}-containing melt, and predominantly Cr^{3+}-bearing phases due to differences in bonding environment between the two phases. Trivalent Cr has high octahedral site preference energy (OSPE) and hence is found solely in VI-fold sites in both minerals and melt (e.g., Berry and O'Neill, 2004). The coordination chemistry of divalent Cr is dictated by its tendency for Jahn-Teller distortions, therefore preferring irregular bonding environments (e.g. Burns, 1975). Indeed, Cr^{2+} is distributed subequally on the M1 and M2 sites of olivine, due to its competing preferences for the larger M2 site and the more distorted M1 site (Li et al., 1995). However, in pyroxenes, the M2 site is both larger and more distorted than the M1, meaning Cr^{2+} is strongly partitioned onto the M2 site (Angel et al., 1989). Its coordination in silicate melts is uncertain, though it may be coordinated by six oxygens in a square planar arrangement (O'Neill and Berry, 2006). Since Cr^{3+} (r = 0.615 Å) exists as 6-fold coordination in all minerals (olivine, pyroxene and spinel) and has shorter M-O distances as compared to Cr^{2+} (r = 0.80 Å), which exists in larger, more distorted geometries, the Cr^{3+} phases should be isotopically heavier. The preferential incorporation of Cr^{3+} into orthopyroxene and Cr-spinel relative to the melt leads to isotope fractionation between them and provides a mechanism to explain the heavier isotopic composition of diogenites compared to the eucrites. In terrestrial peridotites, chromites (which host entirely Cr^{3+}) are isotopically heavier compared to the bulk (Farkaš et al., 2013; Schoenberg et al., 2008), which is further confirmed by the following general $\delta^{53}Cr$ order: chromite-free peridotites (-0.21‰ ~ -0.11‰) < chromite-bearing peridotite (-0.07‰) ≤ chromite (-0.06‰) (Shen et al., 2015) and by

ab initio calculations (Moynier et al., 2011). If a primary melt from the Vestan mantle formed at IW-1, it should only possess ~10% Cr^{3+} (Berry et al., 2006; Wadhwa, 2008). Therefore, the isotopically heavy pyroxenes and spinels in diogenites rapidly uptake most of the limited budget of Cr^{3+} compared to those in eucrites, producing isotopically heavier diogenites.

4.2 The Cr isotopic composition of the bulk Vesta

HED meteorites are likely direct samples from Vesta (McCord et al., 1970; Binzel and Xu, 1993; Russell et al., 2012), but their chemical variation means that estimating the isotopic composition of the Vestan mantle hinges upon identifying samples that have undergone minimal isotopic fractionation relative to their mantle sources. Samples that are most likely to fulfil these criteria are those that represent primary melts, i.e., those in equilibrium with their mantle sources. Among eucrites, the cumulate varieties (including EET 87548) with high Mg#s (54), have accumulated Cr^{3+}-bearing minerals (chromite, pyroxene), that have resulted in an increase in Cr content relative to their parent magma. Because this accumulation could cause Cr isotope fractionation (*cf.* Fig. 1 and section 4.1.), these samples are excluded from the determination of the Vestan mantle composition.

In order to quantify the magnitude of this effect, the *ab-initio* calculations of Moynier et al. (2011) are used to show that chromite should be isotopically heavier than co-existing Cr^{2+}-bearing silicates by about 0.15 ‰ at magmatic temperatures (1200~1400°C; Moynier et al., 2011). The heaviest diogenites have $\delta^{53}Cr$ of -0.07 ‰

381 (LAP 03569 and Johnstone), which are, at most, 0.15 ‰ heavier relative to eucrites. If
382 one considers that a primary melt of the Vestan mantle contains 90% Cr^{2+} (Berry et al.
383 2006), then the diogenites, as cumulates that contain only Cr^{3+}, can represent no greater
384 than 10% by mass of the initial melt. If, in a closed system with a finite Cr budget, the
385 eucrites are complementary to diogenites (which appears not to be the case; Barrat et
386 al. 2008), then they would contain the other 90% of the Cr budget, and the Cr isotope
387 composition of the parental melt would be given by mass balance: $\delta^{53}Cr_{parental}$ =
388 $\delta^{53}Cr_{eucrite} \times 0.9 + \delta^{53}Cr_{diogenite} \times 0.1$, which yields -0.20 ‰, within statistical uncertainty
389 of the eucrite average (-0.22 ± 0.03 ‰).

390 Sample EET 87542 (Mg# = 40) is a petrologically anomalous brecciated eucrite
391 with low Fe/Mn-pyroxene, which underwent unusual subsolidus processing
392 (Mittlefehldt et al., 2015; 2016) that could have modified its Cr isotope composition.
393 Pasamonte has anomalous $\Delta^{17}O$ and hence may not originate from Vesta (Scott et al.,
394 2009), so it cannot be relied upon as a faithful probe of the composition of Vesta. Then,
395 it should be noted that Stannern and Bouvante belong to Stannern Trend, which,
396 although they may indeed be primary Vestan "mantle" melt products, have incorporated
397 crustal material (Barrat et al., 2007) that compromises the degree to which they
398 represent the Vestan mantle and are also excluded. Finally, this leaves three basaltic
399 Main trend basaltic eucrites (Juvinas, Jonzac and Camel Donga, Mg# = 40-42). We
400 assess below whether these samples are representative of their sources.

401 On the basis that many of the main group eucrites' bulk compositions plot near the

1 atm peritectic, saturated in olivine-low Ca pyroxene-plagioclase-spinel-metal, Stolper (1977) made a convincing case for the derivation of these magmas via partial melting of the Vestan mantle. In this model, the most magnesian of these magmas, Sioux County and Juvinas (and similar non-cumulate eucrites with Mg#s ≈ 42), are produced by 15-20% melting, whereas more evolved examples, such as Pasamonte and Nuevo Laredo are liquid residues after moderate degrees (<40%) of fractional crystallization. However, later cosmochemical models postulate Mg#s for the Vestan mantle between 75-80 (Dreibus and Wänke, 1980; Ruzicka et al., 1997). Whether these magmas are representative of the mantle of Vesta can be assessed using K_D Fe-Mg systematics between mafic minerals and melt:

$$K_{D,Min-Melt}^{Fe-Mg} = \frac{\left(\frac{Fe}{Mg}\right)_{Min}}{\left(\frac{Fe}{Mg}\right)_{Melt}}. \quad (4)$$

Experimental studies have shown that this value is close to 0.30 for olivine-melt (Toplis, 2005), orthopyroxene-melt and clinopyroxene-melt (Bédard, 2007; Bédard, 2010). Application of equation (4) results in the expectation that primary melts of the Vestan mantle should have Mg#s between 45 and 55, that is, slightly higher than any of the non-cumulate eucrites (36~42). This was pointed out by (Bartels and Grove, 1991), who suggested that the non-cumulate eucrites may come from a more iron-rich region of the Vestan mantle. Therefore, in lieu of non-cumulate samples that have Mg#s compatible with their direct derivation from mantle representative of bulk silicate Vesta, we adopt the most magnesian eucrites analyzed, Juvinas, Jonzac and Camel Donga, as most representative of Vesta, though the caveats mentioned above should be

considered. From these lines of reasoning we consider bulk silicate Vesta to have $\delta^{53}Cr$ = -0.22 ± 0.03‰.

4.3 Difference in the Cr isotope compositions of Vesta and chondrites caused by evaporation under oxidizing conditions.

Chondrites, commonly considered to be the building blocks of planetary bodies, have homogeneous $\delta^{53}Cr$ within error, with values ranging from -0.05 to -0.15 ‰ (Qin et al., 2015; Bonnand et al., 2016b; Schoenberg et al., 2016) and Cr contents varying from 2650 ppm in CI chondrites to ≈ 3800 ppm in ordinary chondrites (Wasson and Kallemeyn, 1988). Therefore, the choice of a specific chondrite group to represent the composition of Vesta is of secondary importance in discussing the Cr elemental and isotopic disparity between Vesta and its building blocks. However, since ordinary chondrites (OC) possess the closest non-mass dependent Cr and Ti isotopic compositions ($\varepsilon^{54}Cr$ and $\varepsilon^{50}Ti$; Trinquier et al., 2007; 2009; Pedersen et al., 2019) to those of the HED meteorites, it is more logical to treat this group of chondrites as the building blocks of Vesta. Ordinary chondrites with $\delta^{53}Cr$ = -0.12 ± 0.03 ‰ (2SD, N=6; Bonnand et al., 2016b) are isotopically heavier than the estimate of the composition of the bulk silicate Vesta (-0.22 ± 0.03 ‰).

Ordinary chondrites have Cr contents of ~3750 ppm (Kallemeyn et al., 1989). The Cr content of Vesta's mantle is a matter of debate, with estimates of ~ 2300 ppm (Jones, 1984) to ≈ 7000 ppm (see Mandler et al. (2013). As touched upon in section 4.1., the estimate of the Cr content of the Vestan mantle hinges upon the role of Cr-spinel in the

444 melting region; Jones (1984) argues that the experiments of Stolper (1977) predict
445 spinel exhaustion at- or near their liquidus temperatures and hence $D_{Cr} \approx 1$. The models
446 estimating higher Cr content in Dreibus and Wanke (1984); Ruzicka et al. (1997) and
447 Mandler et al. (2013) are predicated on determining the composition of Vesta from
448 binary mixtures of eucrites and diogenites and/or finding the point at which refractory
449 lithophile elements are present in chondritic proportions. This approach implicitly
450 neglects elemental fractionation during partial melting (eucrites) or mineral
451 accumulation (diogenites) and should be treated with caution, and only the model of
452 Jones (1984) considered the behaviour of Cr during partial melting. Additionally, Cr
453 contents upwards of those of chondrites (> 4000 ppm) are difficult to justify given the
454 small size of the Vestan core (Russell et al. 2012). We therefore adopt the estimate of
455 Jones (1984), which is similar to Cr contents of the three representative eucrites
456 (Juvinas-2100 ppm, Jonzac-2501 ppm and Camel donga-2232 ppm). Normalized to Al
457 (a refractory element) and OCs, the fraction (f) of Cr in Vesta is ~0.43 (Al content for
458 Vesta's mantle and OCs are 16941 ppm and 11900 ppm respectively; $f = Cr_{Vesta}/Al_{Vesta}$
459 $/(Cr_{Vesta}/Al_{Vesta} + Cr_{OC}/Al_{OC})$. The origin of this deficit of Cr and the shift toward and
460 enrichment in the lighter Cr isotopes, with a $\Delta^{53}Cr_{Vesta\text{-}OC} = -0.10 \pm 0.04‰$, between
461 Vesta and OC is discussed below (Figure 3).

462 Chromium behaves as a slightly siderophile element under reduced conditions and
463 high temperatures (Wood et al., 2008). Vesta experienced core-mantle differentiation
464 (Russell et al., 2012), which had the potential to cause Cr isotope fractionation (Moynier
465 et al., 2011). Using the parameterization of Siebert et al. (2013), the metal-silicate

partition coefficient (D) of Cr at conditions of core formation on asteroid 4-Vesta (~2000 K and IW-1; pressure effect on Cr partitioning is negligible) is estimated to be $D_{Cr} = 0.11 \pm 0.04$. Considering a core mass fraction of 0.18 for Vesta (Russell et al., 2012) and a bulk silicate Vesta Cr content of 2300 ppm (Jones, 1984), this partitioning value results in a Cr-poor Vestan core containing 262 ± 80 ppm of Cr, which represents roughly 1~3% of the Cr budget of Vesta. Accordingly, the formation of Vesta's core was likely ineffective in producing the Cr depletion or isotope fractionation relative to OCs, particularly when considering the small- to negligible Cr isotope fractionation between metal and silicate at 2000 K (Moynier et al., 2011; Bonnand et al., 2016b).

Thermodynamic modelling shows that high oxygen fugacity, near the FMQ buffer, should be a ubiquitous feature of any silicate melt-vapour disk at high temperatures (>1800 K) (Visscher and Fegley Jr, 2013). These higher oxygen fugacities relative to those of the solar nebular gas promote the evaporation of Cr (Sossi et al. 2019). At these conditions (near FMQ), Cr in the gas should mainly exist as CrO_2 according to calculations made with thermodynamic data for homogeneous equilibria involving Cr, CrO, CrO_2 and CrO_3 gas species from the JANAF tables (Chase, 1998). If we consider that 90% of the Cr in the condensed phase is divalent, the appropriate evaporation equation is:

$$CrO(l) + 1/2O_2 = CrO_2(g). \quad (5)$$

Sossi et al. (2018) estimated the equilibrium fractionation factor of $^{53}Cr/^{52}Cr$ between CrO(l) and CrO_2(g) using bond valence theory to be:

$$\Delta^{53}Cr_{CrO(l)-CrO2(g)} = (-0.31 \pm 0.16) \times \frac{10^6}{T^2} \quad (‰). \quad (6)$$

The composition of the Vestan mantle in equilibrium with a CrO_2-bearing gas phase can be calculated by mass balance in which:

$$\delta^{53}Cr_{vapour} = \frac{\delta^{53}Cr_{system} - \delta^{53}Cr_{silicate\ Vesta} \times f^{Cr}_{silicate\ Vesta}}{(1 - f^{Cr}_{silicate\ Vesta})}. \quad (7)$$

As explained above, $\delta^{53}Cr_{system}$ is taken to be the average of ordinary chondrites (-0.12 ± 0.03 ‰), $\delta^{53}Cr_{silicate\ Vesta}$ is -0.22 ± 0.03 ‰, and $f^{Cr}_{silicate\ Vesta}$ is ~0.43, yielding $\delta^{53}Cr_{vapour}$ = -0.04 ± 0.03‰ and $\Delta^{53}Cr_{CrO(l)-CrO2(g)}$ = -0.18 ± 0.04 ‰. Solving Equation (6) for temperature and propagating uncertainties yields a temperature of 1300 ± 500 K. A similar rationale can be applied using another type of chondrite as representative of bulk Vesta. For example, the most extreme case, using CI chondrites with Cr and Al content of 2630 ppm and 8600 ppm respectively (Wasson and Kallemeyn, 1988) and δ^{53}Cr value of -0.15 ± 0.01 (Bonnand et al., 2016b) gives a $f^{Cr}_{silicate\ Vesta}$ = ~0.44, $\delta^{53}Cr_{vapour}$ = -0.09 ± 0.03 ‰ and $\Delta^{53}Cr_{CrO(l)-CrO2(g)}$ = -0.13 ± 0.04 ‰. According to equation (6), the temperature range is 1550 +750/-600 K (Figure 4). These two extreme models show that the volatile loss of Vesta occurred under relatively cool conditions (<2300 K) and likely near the liquidus of basaltic magma (≈ 1500 K).

These relatively low temperatures for Vesta's volatile loss can be reconciled with a degassing process during a magma ocean stage instead of a high-temperature giant impact (≈ 4000 K; Nakajima and Stevenson, 2014). Volcanic eruptions and magmatic

507 fire fountains may also contribute to volatile loss on a local scale (Day and Moynier,
508 2014). However, the three basaltic eucrites with homogeneous δ^{53}Cr and distinct trace
509 element abundance (Barrat et al., 2000) and different cosmic ray exposure ages (9.5 Ma
510 for Juvinas, 31.4 Ma for Jonzac and 38.5 Ma for Camel Donga; Eugster and Michel,
511 1995) most probably come from different regions of Vesta, so localized degassing
512 processes are not consistent with the Cr isotopic data. Furthermore, considering that the
513 volatile degassing process must occur before Vestan crust formation, magmatic
514 degassing should predate the magmatic differentiation of the HEDs that lead to co-
515 variations between δ^{53}Cr and Mg# between eucrites and diogenites.

516 The homogeneous oxygen isotope compositions in HEDs suggests a widespread
517 magma ocean on Vesta (Greenwood et al., 2005; 2014), which is consistent with the Cr
518 isotopic evidence in this study. Al-Mg and Mn-Cr ages for bulk HED meteorites
519 indicate that Vesta differentiated very early, 1~3 Ma after CAIs (the first solids formed
520 in the Solar System), and these old Al-Mg and Mn-Cr ages should reflect the crust-
521 mantle differentiation after early magma ocean (Trinquier et al., 2008; Schiller et al.,
522 2011; Day et al., 2012; Hublet et al., 2017; Schiller et al., 2017). An early-formed
523 carapace or shell formed via radiative cooling from the surface could effectively shut-
524 off evaporation, however, numerical calculations show that these skins are of the order
525 of a few centimeters thick and prone to foundering (Hin et al. 2017), and therefore do
526 not restrict outgassing from small rocky bodies. As such, the late formation of the
527 Vestan crust shows that the volatile depletion on Vesta must have occurred before the
528 crystallization of the magma ocean, which is consistent with volatile loss ages, within

1 My after CAI, suggested from Rb-Sr dating (Hans et al., 2013) and with the heavy Mg isotope enrichment observed (Hin et al., 2017; Dhaliwal et al., 2018). However, the magma ocean model is challenged by considering the physical principles of planetary accretion and geochemical and petrological evidence from meteorites (Lunning et al., 2015; Wilson and Keli, 2017), which suggest that magma oceans are not ubiquitous occurrence during planetary formation. If so, then the volatile depletion of Vesta may have been imposed by accretion of material depleted in the solar nebula (Bloom et al., 2018). However, the nebular gas is very reduced (with $\log fO_2$ = -18.1 at 1500 K, or IW-6.8; Grossman et al. 2008), and under such conditions, neither Mn nor Cr are appreciably volatile. It would therefore be difficult to explain the super-chondritic Mn/Na of Vesta (O'Neill and Palme, 2008). Furthermore, Cr in condensed phases would be expected to be, on average, more oxidized (a combination of Cr^{2+} and Cr metal) relative to the gas phase (Cr^0), such that equilibrium isotope fractionation would result in heavy Cr in the solid residue. In this way, Cr in Vesta should be isotopically heavier than chondrites, which is not consistent with the light Cr isotope compositions in HEDs. As highlighted above, it cannot be excluded that the eucrites come from a fractionated, Fe-rich part of the Vestan mantle, or that there is resolvable Cr isotope fractionation during partial melting. Finally, the Cr isotopic study in eucrites and diogenites supports the large-scale magma ocean caused the volatile depletion, and magma oceans should play a critical role in determining the volatile element contents of bodies formed in the early Solar System (Hin et al. 2017; Dhaliwal et al. 2018; Young et al. 2019).

5 Conclusions

This work reports high-precision Cr stable isotope compositions of bulk eucrites and diogenites. It shows that eucrites are isotopically lighter than diogenites, and that their Cr isotope compositions are correlated with the Cr content and Mg#, which suggests crystallization modified the Cr isotope composition of magmas on Vesta. This systematics is reconciled with isotopically heavy Cr^{3+} entering orthopyroxene that characterizes diogenites, whereas the eucrites represent both parental partial melts of the Vestan mantle, and some later differentiates that contain predominantly Cr^{2+}.

Based on their high Mg#s and lack of accumulated minerals, the non-cumulate eucrites likely provide the best indication as to the composition of the mantle of Vesta. However, the Cr isotope composition deduced for Vesta based on these samples (-0.22 ± 0.03 ‰) is lighter than that of its potential building blocks, ordinary chondrites (-0.12 ± 0.03 ‰). This deficit may arise due to *i)* partial melting in which residual Cr^{3+}-bearing phases in the Vestan mantle sequester the heavy isotopes or *ii*) vapor loss during equilibrium with a magma ocean on Vesta. The former requires very high Cr contents in the Vestan mantle, and that partial melting occurred at oxygen fugacities high enough to stabilize chromite in the mantle source. By contrast, equilibrium fractionation of Cr isotopes necessitates an oxidized vapor and reduced residue, consistent with thermodynamic constraints of the composition of the vapor phase above a silicate magma ocean. If correct, this model suggests a relatively low temperature for the volatile degassing process (< 2300 K) that lead to the impoverishment and light isotope

572 composition of Cr. This result argues that magma ocean degassing may be ubiquitous

573 during the accretionary stages of small telluric bodies.

574

Acknowledgements

We thank the ERC under the European Community's H2020 framework program/ERC grant agreement (no. 637503, Pristine) and the French National Research Agency (ANR) for a Chaire d'Excellence Sorbonne Paris Cité (no. IDEX13C445) and for the UnivEarthS Labex program (no. ANR-10-LABX-0023 and ANR-11-IDEX-0005-02). Parts of this work were supported by IPGP multidisciplinary program PARI, and by Region île-de-France SESAME Grant (no. 12015908). Julien Siebert acknowledges funding from the ANR project VolTerre (no. ANR-14-CE33-0017-01). Assistance on mass spectrometry from Pascale Louvat was also appreciated. We are also grateful to insightful comments from Martin Schiller, James Day and another two anonymous reviewers and editorial handling by Associate Editor James Day and Guest Editor Mahesh Anand. Ke Zhu acknowledges a Ph.D. fellowship from China Scholarship Council (no. 201706340161).

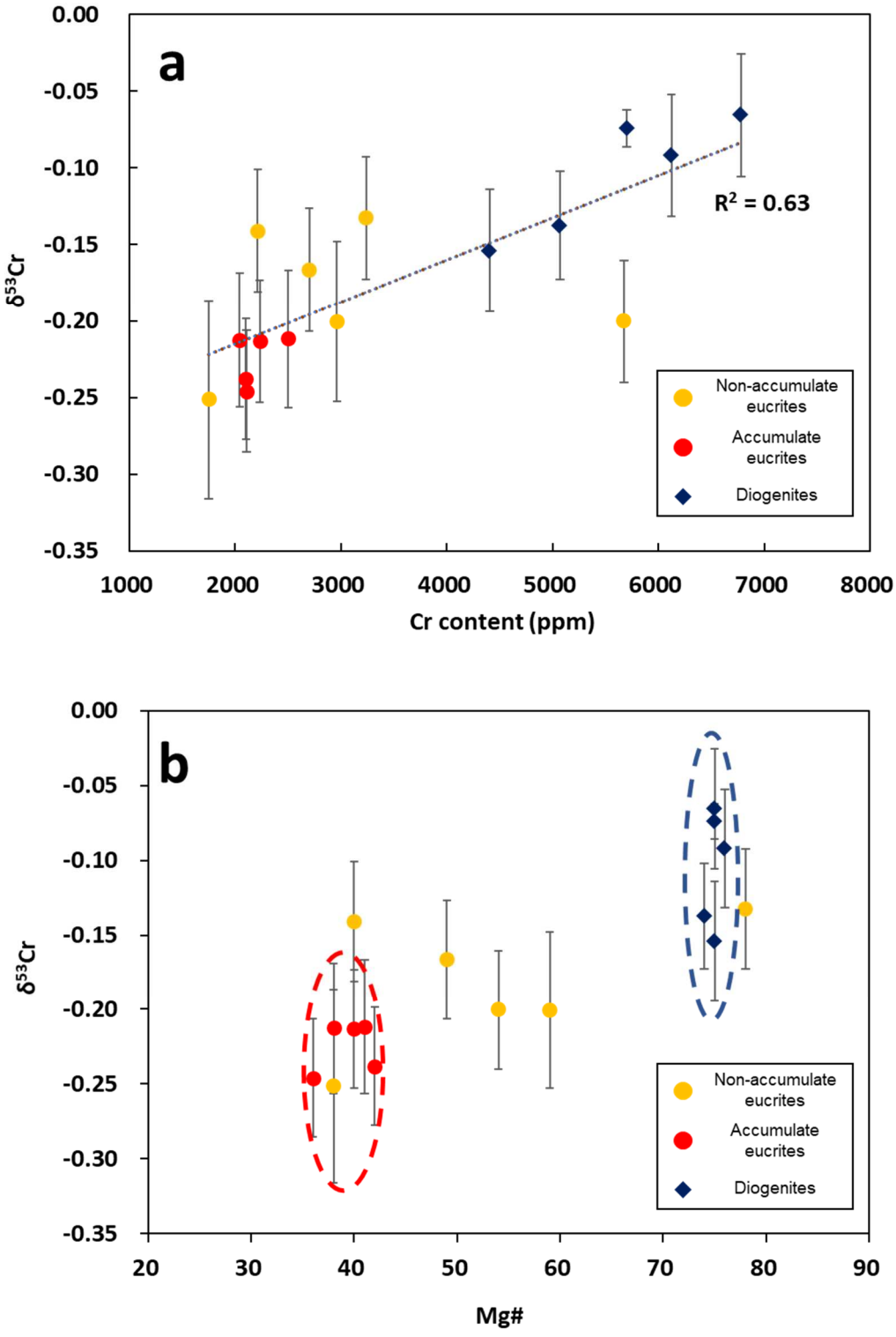

Figure 1 a. Chromium isotope composition vs. Cr content in HED samples. b. Cr isotopes composition vs. Mg# in HED samples. Red circles: non-accumulate eucrites, yellow circles: cumulate eucrites and blue diamonds: diogenites. The red circle indicates the reservoir for basaltic eucrites with low Mg# and light Cr, while the blue circle is for the diogenites with high Mg# and isotopically heavy Cr.

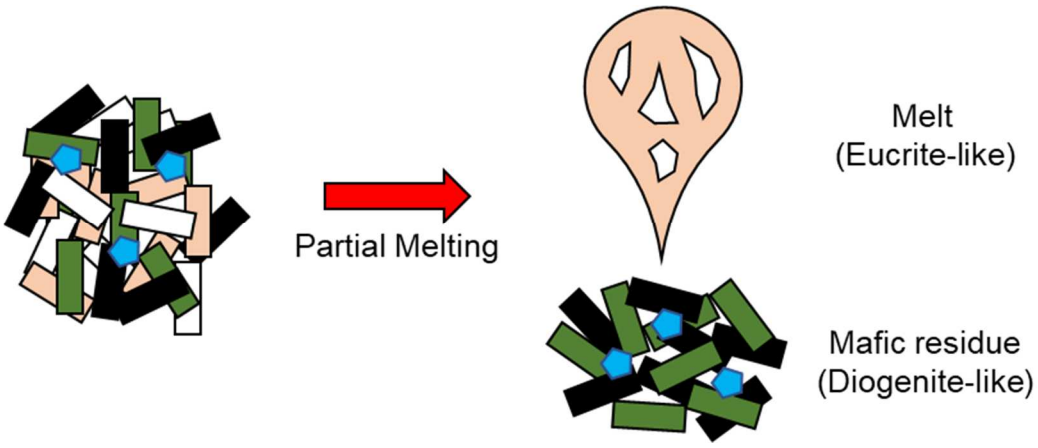

Figure 2 Schematic diagram illustrates the effect of partial melting on the Cr stable isotope composition of Vesta. The white and light pink bars are felsic composition, while the green and black bars represent the mafic composition. The blue pentagons are chromites (Cr-spinels). After partial melting, the felsic composition would mainly go to the melt while the mafic composition would stay in the residues. It should be noted that, the pyroxenes and chromites which are compatible to isotopically heavy Cr^{3+} in the residues would make the residue have higher Cr^{3+}/Cr_{Total} and isotopically heavy for Cr isotopes. Complementarily, the melt part would be dominated in Cr^{2+} and isotopically light for Cr. However, the diogenites are not necessarily complementary to eucrites, but some other range of Vestan melts.

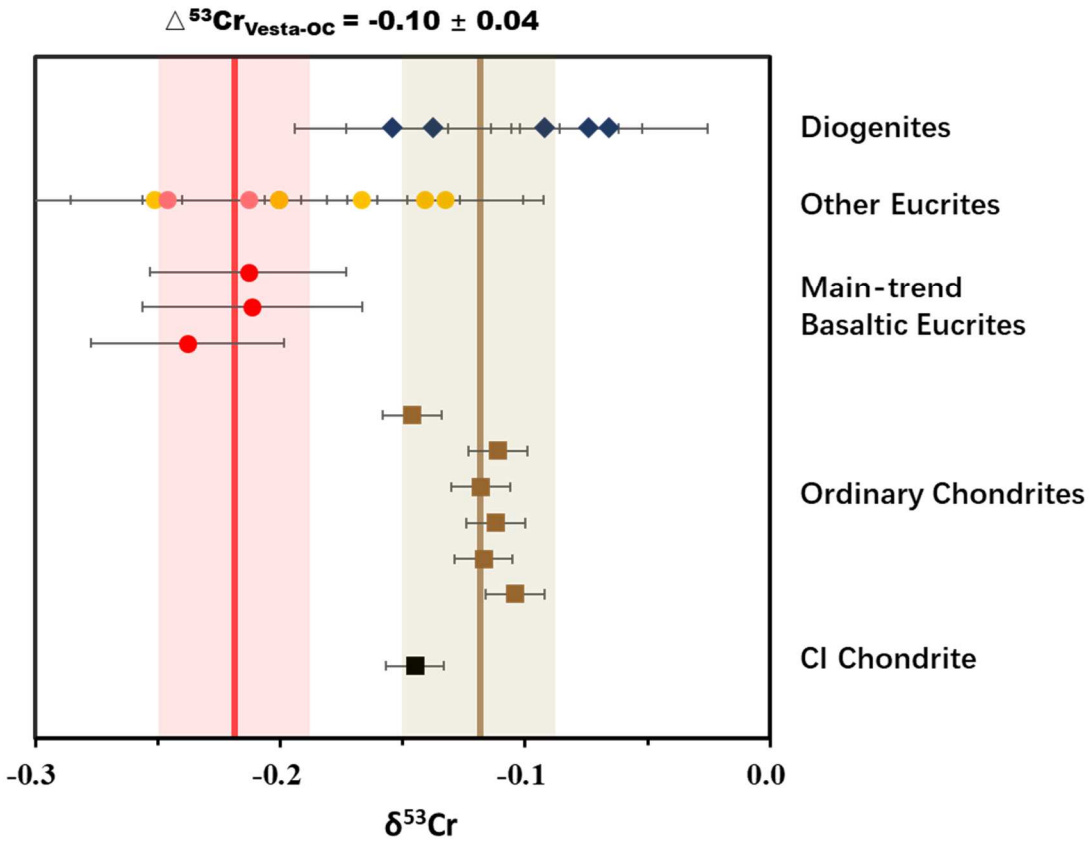

Figure 3 Comparison of the Cr isotope compositions of Diogenites (blue diamond), Eucrites (yellow and red circles). The red is for main-trend basaltic eucrites, and the pink is for Stannern-trend basaltic eucrites and yellow for other eucrites). Ordinary chondrites are shown as brown squares and CI chondrite is shown as a black square. The light red shade indicates the 2SD of Cr isotope values for three basaltic eucrites which may represent the primitive Vesta, while the light brown shade is for that of ordinary chondrites which may represent the building blocks for Vesta. The $\delta^{53}Cr$ deficit between primitive Vesta and ordinary chondrites is $\Delta^{53}Cr_{Vesta\text{-}OC} = -0.10 \pm 0.04$, which should be equilibrium fractionation during the Cr loss or caused by partial melting effect at a large-scale magma ocean stage.

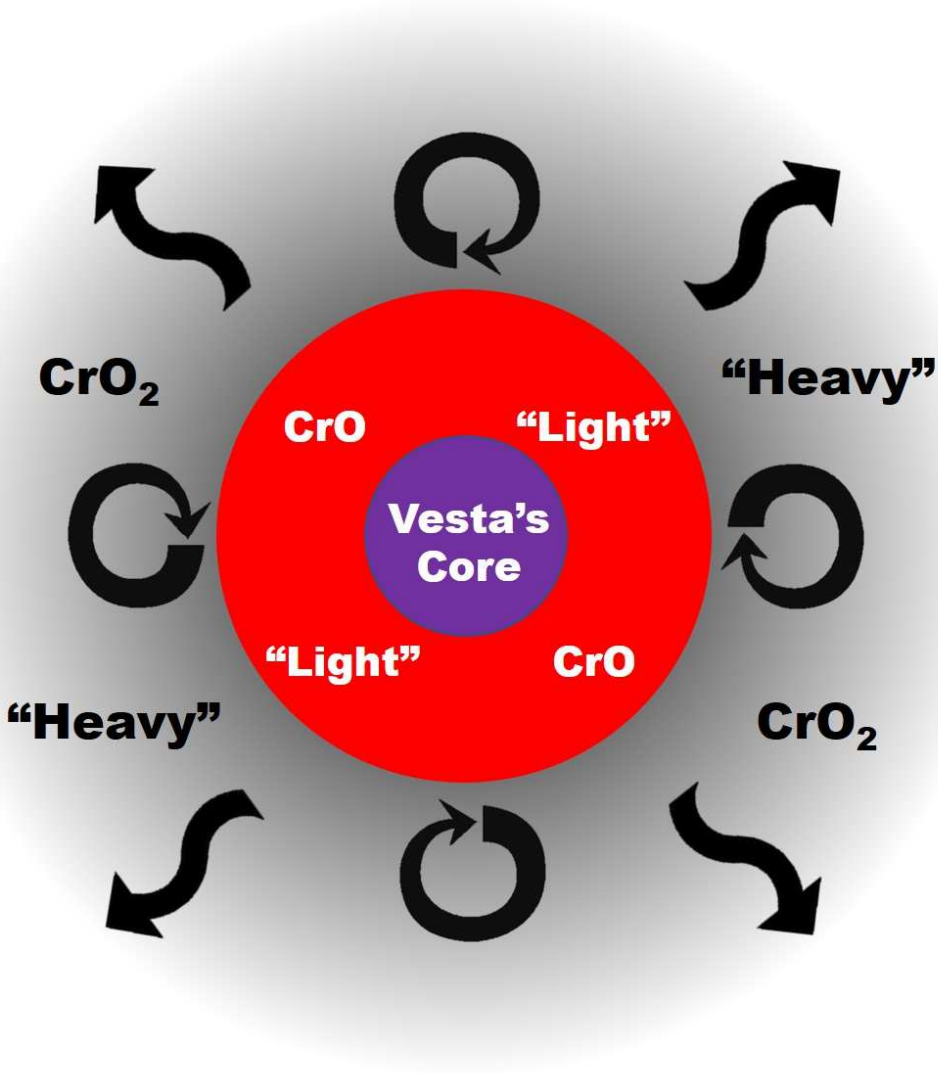

Figure 4 Schematic diagram illustrating the effect of volatile loss on the Cr stable isotope composition of Vesta (average radius of 262.7 km; Russell et al., 2012). In this model, within 1 Myr after CAI (dated by the volatile-sensitive ^{87}Rb-^{87}Sr chronometer; Hans et al., 2013), the ^{26}Al-to-^{26}Mg decay system released sufficient heat to melt Vesta globally (Schiller et al., 2011). The temperature at the surface of the magma ocean is estimated to have been under 2300 K. Under such conditions, the fO_2 during silicate-vapor equilibrium should approach the FMQ buffer. Modeling in Young et al. (2019) support near-equilibrium isotope fractionation between a magma ocean and its vapour atmosphere during planetesimal evaporation. At this fO_2, Cr in the vapour (CrO_2) is more oxidized than in the melt at equilibrium (CrO). Accordingly, equilibrium fractionation produces a residual melt isotopically lighter than the vapour. The core only contains 1~3% of Vesta's Cr budget, and core formation likely did not induce Cr isotope fractionation.

641 Table 1 Cr stable isotope, Cr content and Mg# data of HED meteorites

Sample	Fall/Find	Type	Cr (ppm)	Mg#	δ^{53}Cr	2SD	N
Pasamonte	fall	Eucrite-pmict	1750	38	-0.27	0.06	2
replicate					-0.23	0.05	2
average					-0.25	0.06	4
Stannern	fall	Eucrite-mmict	2041	38	-0.22	0.04	2
replicate					-0.21	0.04	2
average					-0.21	0.04	4
Jonzac	fall	Eucrite-mmict	2501	41	-0.21	0.04	2
replicate					-0.22	0.04	2
average					-0.21	0.04	4
Juvinas	fall	Eucrite-mmict	2100	42	-0.26	0.04	2
replicate					-0.22	0.04	2
average					-0.24	0.04	4
Bouvante	find	Eucrite-mmict	2106	36	-0.25	0.04	2
Camel Donga	find	Eucrite-mmict	2232	40	-0.21	0.04	2
Moore County	fall	Eucrite-cm	2699	49	-0.17	0.04	2
Pomozdino	find	Eucrite-cm	3237	78	-0.13	0.04	2
Serra de Magé	fall	Eucrite-cm	2962	59	-0.20	0.05	2
EET 87548	find	Eucrite-Mg rich	5673	54	-0.20	0.04	4
EET 87542	find	Eucrite-br	2212	40	-0.14	0.04	2
EET 79002	find	Diogenite	5068	74	-0.14	0.04	2
Tatahouine	fall	Diogenite	6122	76	-0.09	0.04	2
LAP 03569	find	Diogenite	6780	75	-0.07	0.04	2
Shalka	fall	Diogenite	4404	75	-0.15	0.04	4
Johnstown*	fall	Diogenite	5700	75	-0.07	0.01	1
BHVO-2		Basalt	280		-0.13	0.04	1
DTS-1		Dunite	3990		-0.08	0.04	2
PCC-1		Peridotite	2730		-0.10	0.04	2

642 Note: the Cr content and Mg# (the ratio of Mg to the sum of Mg and Fe on an atomic
643 basis) data are in these literature (Barrat et al., 2000; 2008; Bonnand et al., 2016b;
644 Lugmair and Shukolyukov, 1998; Schoenberg et al., 2016; Warren et al., 2009). One
645 data marked * (Johnstone) is from Bonnand et al. (2016b).
646

References

Angel, R., Gasparik, T. and Finger, L. (1989) Crystal structure of a Cr^{2+}-bearing pyroxene. *Am. Mineral.* **74**, 599-603.

Barrat, J.-A., Blichert-Toft, J., Gillet, P. and Keller, F. (2000) The differentiation of eucrites: the role of in situ crystallization. *Meteorit. Planet. Sci.* **35**, 1087-1100.

Barrat, J.-A., Yamaguchi, A., Greenwood, R., Bohn, M., Cotten, J., Benoit, M. and Franchi, I. (2007) The Stannern trend eucrites: Contamination of main group eucritic magmas by crustal partial melts. *Geochim. Cosmochim. Acta* **71**, 4108-4124.

Barrat, J.-A., Yamaguchi, A., Greenwood, R., Benoit, M., Cotten, J., Bohn, M. and Franchi, I. (2008) Geochemistry of diogenites: Still more diversity in their parental melts. *Meteorit. Planet. Sci.* **43**, 1759-1775.

Bartels, K. and Grove, T. (1991) High-pressure experiments on magnesian eucrite compositions-Constraints on magmatic processes in the eucrite parent body. *Proc. Lunar Planet. Sci.* **21**, 351-365.

Beck, A.W. and McSween, H.Y. (2010) Diogenites as polymict breccias composed of orthopyroxenite and harzburgite. *Meteorit. Planet. Sci.* **45**, 850-872.

Beck, P., Barrat, J.A., Grisolle, F., Quirico, E., Schmitt, B., Moynier, F., Gillet, P. and Beck, C. (2011) NIR spectral trends of HED meteorites: Can we descriminate between the magmatic evolution, mechanical mixing and observation geometry effects? *Icarus* **215**, 560-571

Bédard, J.H. (2007). Trace element partitioning coefficients between silicate melts and orthopyroxene: Parameterizations of D variations. *Chem. Geol.* **244**, 263-303.

Bédard, J.H. (2010) Parameterization of the Fe=Mg exchange coefficient (K_d) between clinopyroxene and silicate melts. *Chem. Geol.* **274**, 169-176.

Bell, A. S., Burger, P. V., Le, L., Shearer, C. K., Papike, J. J., Sutton, S. R., Newville M. and Jones, J. (2014). XANES measurements of Cr valence in olivine and their applications to planetary basalts. *Am. Mineral.* **99**, 1404-1412.

Berry, A.J. and O'Neill, H.S.C. (2004) A XANES determination of the oxidation state of chromium in silicate glasses. *Am. Mineral.* **89**, 790-798.

Berry, A.J., O'Neill, H.S.C., Scott, D.R., Foran, G.J. and Shelley, J. (2006) The effect of composition on Cr^{2+}/Cr^{3+} in silicate melts. *Am. Mineral.* **91**, 1901-1908.

Binzel, R.P. and Xu, S. (1993) Chips off of Asteroid 4 Vesta: Evidence for the Parent Body of Basaltic Achondrite Meteorites. *Science* **260**, 186-191.

Bloom, H.E., Chen, H., Fegley, B., Lodders, K., and Wang, K. (2018). Potassium Isotope Compositions of Carbonaceous and Ordinary Chondrites: Implications on the Origin of Volatile Depletion in the Early Solar System. *49th Lunar Planet. Sci. Conf. Texas.* #1193 (abstr.)

Bonnand, P., Parkinson, I.J. and Anand, M. (2016a) Mass dependent fractionation of stable chromium isotopes in mare basalts: Implications for the formation and the differentiation of the Moon. *Geochim. Cosmochim. Acta* **175**, 208-221.

Bonnand, P., Williams, H.M., Parkinson, I.J., Wood, B.J. and Halliday, A.N. (2016b) Stable chromium isotopic composition of meteorites and metal–silicate experiments: Implications for fractionation during core formation. *Earth Planet. Sci. Lett.* **435**, 14-21.

Bowman, L., Spilde, M. and Papike, J. (1997) Automated energy dispersive spectrometer modal

689 analysis applied to the diogenites. *Meteorit. Planet. Sci.* **32**, 869-875.
690 Boyce, J.W., Treiman, A.H., Guan, Y., Ma, C., Eiler, J.M., Gross, J., Greenwood, J.P. and Stolper,
691 E.M. (2015) The chlorine isotope fingerprint of the lunar magma ocean. *Sci. adv.* **1**, e1500380.
692 Boyce, J. W., Kanee, S. A., McCubbin, F. M., Barnes, J. J., Bricker, H., and Treiman, A. H.
693 (2018). Early loss, fractionation, and redistribution of chlorine in the Moon as revealed by the
694 low-Ti lunar mare basalt suite. *Earth Planet. Sci. Lett.* **500**, 205-214.
695 Burns, R.G. (1975) On the occurrence and stability of divalent chromium in olivines included in
696 diamonds. Contrib. *Mineral. Petrol.* **51**, 213-221.
697 Chase, M. (1998) NIST—JANAF Thermochemical Tables (Journal of Physical and Chemical
698 Reference Data Monograph No. 9). *American Institute of Physics.*
699 Chen, G., Bai, Y., Zeng, R. J., and Qin, L. (2019). Effects of different metabolic pathways and
700 environmental parameters on Cr isotope fractionation during Cr (VI) reduction by extremely
701 thermophilic bacteria. *Geochimica et Cosmochimica Acta*. **256**, 135-146.
702 Day, J.M.D., Walker, R.J., Qin, L. and Rumble III, D. (2012) Late accretion as a natural
703 consequence of planetary growth. *Nature Geoscience* **5**, 614-617.
704 Day, J.M.D. and Moynier, F. (2014) Evaporative fractionation of volatile stable isotopes and their
705 bearing on the origin of the Moon. *Phil. Trans. R. Soc. A.* **372**, 20130259.
706 Delaney, J.S., Prinz, M. and Takeda, H. (1984) The polymict eucrites. *Journal of Geophysical*
707 *Research: Solid Earth* **89**, C251-C288.
708 Dhaliwal, J.K., Day, J.M.D. and Moynier F. (2018) Volatile element loss during planetary magma
709 ocean phases. *Icarus* **300**, 249-260.
710 Dreibus, G. and Wänke, H. (1980) The bulk composition of the eucrite parent asteroid and its
711 bearing on planetary evolution. *Zeitschrift für Naturforschung A* **35**, 204-216.
712 Eugster, O., and Michel, T. (1995). Common asteroid break-up events of eucrites, diogenites,
713 and howardites and cosmic-ray production rates for noble gases in achondrites. *Geochimica et*
714 *Cosmochimica Acta*. **59**, 177-199.
715 Farkaš, J., Chrastný, V., Novák, M., Čadkova, E., Pašava, J., Chakrabarti, R., Jacobsen, S.B.,
716 Ackerman, L. and Bullen, T.D. (2013) Chromium isotope variations ($\delta^{53/52}$Cr) in mantle-derived
717 sources and their weathering products: Implications for environmental studies and the evolution
718 of $\delta^{53/52}$Cr in the Earth's mantle over geologic time. *Geochim. Cosmochim. Acta* **123**, 74-92.
719 Greenwood, R.C., Franchi, I.A., Jambon, A. and Buchanan, P.C. (2005) Widespread magma
720 oceans on asteroidal bodies in the early solar system. *Nature* **435**, 916-918.
721 Greenwood, R.C., Franchi, I.A., Scott, E.R.D., Barrat, J.A. and Norman, M. (2009) Oxygen
722 Isotope Variation in the HEDs: How Homogeneous is Vesta? *72nd Annual Meteoritical Society*
723 *Meeting*, Nancy. #5436 (abstr.).
724 Greenwood, R.C., Barrat, J.-A., Yamaguchi, A., Franchi, I.A., Scott, E.R., Bottke, W.F. and
725 Gibson, J.M. (2014) The oxygen isotope composition of diogenites: Evidence for early global
726 melting on a single, compositionally diverse, HED parent body. *Earth Planet. Sci. Lett.* **390**,
727 165-174.
728 Grossman, L., Beckett, J. R., Fedkin, A. V., Simon, S. B., & Ciesla, F. J. (2008). Redox
729 conditions in the solar nebula: Observational, experimental, and theoretical constraints.
730 *Reviews in Mineralogy and Geochemistry* **68**, 93-140.
731 Hans, U., Kleine, T. and Bourdon, B. (2013) Rb–Sr chronology of volatile depletion in
732 differentiated protoplanets: BABI, ADOR and ALL revisited. *Earth Planet. Sci. Lett.* **374**, 204-

214.
Hin, R., Coath, C.D., Carter, P.J., Nimmo, F., Laim Y.J., Pogge Von Strandman, P., Willbold, M., Leinhardt, Z., Walter, M. and Elliot, T. Magnesium isotopic evidence that vapour loss shapes planetary composition. *Nature* **549**, 511-515.
Hublet, G., Debaille, V., Wimpenny, J. and Yin, Q.Z. (2017) Differentiation and magmatic activity in Vesta evidenced by ^{26}Al-^{26}Mg dating in eucrites and diogenites. *Geochim. Cosmochim. Acta* **218**, 73-97.
Jones, J.H. (1984) The composition of the mantle of the eucrite parent body and the origin of eucrites. *Geochim. Cosmochim. Acta* **48**, 641-648.
Kallemeyn, G.W., Rubin, A.E., Wang, D. and Wasson, J.T. (1989) Ordinary chondrites: Bulk compositions, classification, lithophile-element fractionations and composition-petrographic type relationships. *Geochim. Cosmochim. Acta* **53**, 2747-2767.
Karner, J., Papike, J., Shearer, C., McKay, G., Le, L. and Burger, P. (2007) Valence state partitioning of Cr and V between pyroxene-melt: Estimates of oxygen fugacity for martian basalt QUE 94201. *Am. Mineral.* **92**, 1238-1241.
Kato, C., Moynier, F., Valdes, M.C., Dhaliwal, J.K. and Day, J.M.D. (2015) Extensive volatile loss during formation and differentiation of the Moon. *Nat. Commun.* **6**, 7617.
Kato, C. and Moynier, F. (2017) Gallium isotopic evidence for extensive volatile loss from the Moon during its formation. *Sci. Adv.* **3**, e1700571.
Keil, K. (2002) Geological history of asteroid 4 Vesta: The "smallest terrestrial planet". *Asteroids III* (eds. W. F. Bottke et al.) Univ. of Arizona Press, Tucson, pp. 573-584.
Lamoreaux R H, Hildenbrand D L. (1984) High temperature vaporization behavior of oxides. I. Alkali metal binary oxides. *Journal of physical and chemical reference data.* **13**, 151-173.
Lamoreaux R.H., Hildenbrand D.L. and Brewer L. (1987) High-Temperature Vaporization Behavior of Oxides II. Oxides of Be, Mg, Ca, Sr, Ba, B, Al, Ga, In, Tl, Si, Ge, Sn, Pb, Zn, Cd, and Hg. *Journal of physical and chemical reference data*. **16**, 419-443.
Li, J., O'Neil, H.S.C. and Seifert, F. (1995) Subsolidus Phase Relations in the System MgO-SiO_2-Gr-O in Equilibrium with Metallic Cr, and their Significance for the Petrochemistry of Chromium. *J. Petrol.* **36**, 107-132.
Lugmair, G. and Shukolyukov, A. (1998) Early solar system timescales according to ^{53}Mn-^{53}Cr systematics. *Geochim. Cosmochim. Acta* **62**, 2863-2886.
Lunning, N. G., McSween, H. Y., Tenner, T. J., Kita, N. T. and Bodnar, R. J. (2015). Olivine and pyroxene from the mantle of asteroid 4 Vesta. *Earth Planet. Sci. Lett.* **418**, 126-135.
Magna, T., Šimčíková, M. and Moynier, F. (2014) Lithium systematics in howardite–eucrite–diogenite meteorites: Implications for crust–mantle evolution of planetary embryos. *Geochim. Cosmochim. Acta* **125**, 131-145.
Mallmann, G. and O'Neill, H.S.C. (2009) The crystal/melt partitioning of V during mantle melting as a function of oxygen fugacity compared with some other elements (Al, P, Ca, Sc, Ti, Cr, Fe, Ga, Y, Zr and Nb). *J. Petrol.* **50**, 1765-1794.
Mandler, B.E. and Elkins‐Tanton, L.T. (2013) The origin of eucrites, diogenites, and olivine diogenites: Magma ocean crystallization and shallow magma chamber processes on Vesta. *Meteorit. Planet. Sci.* **48**, 2333-2349.
Mann, U., Frost, D. J., & Rubie, D. C. (2009) Evidence for high-pressure core-mantle

776 differentiation from the metal–silicate partitioning of lithophile and weakly-siderophile elements.
777 *Geochim. Cosmochim. Acta* **73**, 7360-7386.
778 Mason, B. (1967) Meteorites. *American Scientist*. **55**, 429-455.
779 Mayne, R.G., McSween Jr, H.Y., McCoy, T.J., and Gale, A. (2009) Petrology of the unbrecciated
780 eucrites. *Geochim. Cosmochim. Acta* **73**, 794-819.
781 McCord, T.B., Adams, J.B. and Johnson, T.V. (1970) Asteroid Vesta: Spectral reflectivity and
782 compositional implications. *Science* **168**, 1445-1447.
783 Mittlefehldt, D.W. (2014) 1.6 - Achondrites A2 - Holland, Heinrich D, in: Turekian, K.K. (Ed.),
784 *Treatise on Geochemistry (Second Edition).* Elsevier, Oxford, pp. 235-266.
785 Mittlefehldt, D.W. (2015) Asteroid (4) Vesta: I. The howardite-eucrite-diogenite (HED) clan of
786 meteorites. *Chem. Erde* **75**, 155-183.
787 Mittlefehldt, D.W., Peng, Z.X. and Ross, D.K. (2015) Petrology of Anomalous Eucrites, *46th*
788 *Lunar Planet. Sci. Conf.* Texas. #1933 (abstr.).
789 Mittlefehldt, D.W., Peng, Z.X. and Mertzman, S.A. (2016) Compositions of Normal and
790 Anomalous Eucrite-Type Mafic Achondrites, *79th Annual Meeting of the Meteoritical Society.*
791 Berlin. #6324 (abstr.).
792 Mougel, B., Moynier, F., Göpel, C. and Koeberl, C. (2017) Chromium isotope evidence in ejecta
793 deposits for the nature of Paleoproterozoic impactors. *Earth Planet. Sci. Lett.* **460**, 105-111.
794 Mougel, B., Moynier, F. and Göpel, C. (2018) Chromium isotopic homogeneity between the
795 Moon, the Earth, and enstatite chondrites. *Earth Planet. Sci. Lett.* **481**, 1-8.
796 Moynier, F., Yin, Q.-Z. and Schauble, E. (2011) Isotopic evidence of Cr partitioning into Earth's
797 core. *Science* **331**, 1417-1420.
798 Moynier, F., Day, J.M.D., Okui, W., Yokoyama, T., Bouvier, A., Walker, R.J. and Podosek, F.A.
799 (2012) Planetary-scale strontium isotopic heterogeneity and the age of volatile depletion of
800 early Solar System materials. *Astrophys. J.* **758**, 45.
801 Nakajima, M. and Stevenson, D.J. (2014) Investigation of the initial state of the Moon-forming
802 disk: Bridging SPH simulations and hydrostatic models. *Icarus* **233**, 259-267.
803 O'Neill, H.S.C. and Berry, A.J. (2006) Activity coefficients at low dilution of CrO, NiO and CoO
804 in melts in the system CaO–MgO–Al_2O3–SiO_2 at 1400°C: Using the thermodynamic behaviour
805 of transition metal oxides in silicate melts to probe their structure. *Chem. Geol.* **231**, 77-89.
806 O'Neill, H.S.C. and Palme, H. (2008) Collisional erosion and the non-chondritic composition of
807 the terrestrial planets. *Philos. Trans. Roy. Soc. Lond.* A **366**, 4205-4238.
808 Paniello, R.C., Day, J.M.D. and Moynier, F. (2012a) Zinc isotopic evidence for the origin of the
809 Moon. *Nature* **490**, 376.
810 Paniello, R.C., Moynier, F., Beck, P., Barrat, J.-A., Podosek, F.A. and Pichat, S. (2012b) Zinc
811 isotopes in HEDs: Clues to the formation of 4-Vesta, and the unique composition of Pecora
812 Escarpment 82502. *Geochim. Cosmochim. Acta* **86**, 76-87.
813 Pedersen, S. G., Schiller, M., Connelly, J. N., and Bizzarro, M. (2019). Testing accretion
814 mechanisms of the H chondrite parent body utilizing nucleosynthetic anomalies. *Meteorit.*
815 *Planet. Sci*. in press. https://doi.org/10.1111/maps.13269
816 Pringle, E.A., Savage, P.S., Badro, J., Barrat, J.A., and Moynier, F. (2013) Redox state during
817 core formation on asteroid 4-Vesta. *Earth Planet. Sci. Lett.* **373**, 75-82.
818 Pringle, E.A. and Moynier, F. (2017) Rubidium isotopic composition of the Earth, meteorites,
819 and the Moon: Evidence for the origin of volatile loss during planetary accretion. *Earth Planet.*

Sci. Lett. **473**, 62-70.
Qin, L., Xia, J., Carlson, R. and Zhang, Q. (2015) Chromium stable isotope composition of meteorites, *46th Lunar Planet. Sci. Conf.* Texas. #2015 (abstr.).
Rammensee, W., Palme, H., & Wanke, H. (1983). Experimental investigation of metal-silicate partitioning of some lithophile elements (Ta, Mn, V, Cr). *Lunar Planet. Sci. Conf.* **14**, 628-629. (abstr.).
Righter, K. and Drake, M.J. (1997) A magma ocean on Vesta: Core formation and petrogenesis of eucrites and diogenites. *Meteorit. Planet. Sci.* **32**, 929-944.
Righter, K., Sutton, S.R., Danielson, L., Pando, K. and Newville, M. (2016) Redox variations in the inner solar system with new constraints from vanadium XANES in spinels. *Am. Mineral.* **101**, 1928-1942.
Roeder, P. and Reynolds, I. (1991) Crystallization of chromite and chromium solubility in basaltic melts. *J. Petrol.* **32**, 909-934.
Russell, C., Raymond, C., Coradini, A., McSween, H., Zuber, M.T., Nathues, A., De Sanctis, M.C., Jaumann, R., Konopliv, A. and Preusker, F. (2012) Dawn at Vesta: Testing the protoplanetary paradigm. *Science* **336**, 684-686.
Ruzicka, A., Snyder, G.A. and Taylor, L.A. (1997) Vesta as the howardite, eucrite and diogenite parent body: Implications for the size of a core and for large-scale differentiation. *Meteorit. Planet. Sci.* **32**, 825-840.
Sanborn, M.E. and Yin, Q.-Z. (2014) Chromium Isotopic Composition of the Anomalous Eucrites: An Additional Geochemical Parameter for Evaluating Their Origin, *45th Lunar Planet. Sci. Conf.* Texas. #2018. (abstr.).
Sarafian, A.R., John, T., Roszjar, J. and Whitehouse, M.J. (2017) Chlorine and hydrogen degassing in Vesta's magma ocean. *Earth Planet. Sci. Lett.* **459**, 311-319.
Schiller, M., Baker, J., Creech, J., Paton, C., Millet, M.-A., Irving, A. and Bizzarro, M. (2011) Rapid timescales for magma ocean crystallization on the howardite-eucrite-diogenite parent body. *Astrophys. J. Lett.* **740**, L22.
Schiller M, Connelly J N, Bizzarro M. (2017) Lead and Mg isotopic age constraints on the evolution of the HED parent body. *Meteorit. Planet. Sci.* **52**: 1233-1243.
Schoenberg, R., Zink, S., Staubwasser, M. and Von Blanckenburg, F. (2008) The stable Cr isotope inventory of solid Earth reservoirs determined by double spike MC-ICP-MS. *Chem. Geol.* **249**, 294-306.
Schoenberg, R., Merdian, A., Holmden, C., Kleinhanns, I.C., Haßler, K., Wille, M. and Reitter, E. (2016) The stable Cr isotopic compositions of chondrites and silicate planetary reservoirs. *Geochim. Cosmochim. Acta* **183**, 14-30.
Scott, E.R., Greenwood, R.C., Franchi, I.A. and Sanders, I.S. (2009) Oxygen isotopic constraints on the origin and parent bodies of eucrites, diogenites, and howardites. *Geochim. Cosmochim. Acta* **73**, 5835-5853.
Sharp, Z., Shearer, C., McKeegan, K., Barnes, J. and Wang, Y. (2010) The chlorine isotope composition of the Moon and implications for an anhydrous mantle. *Science* **329**, 1050-1053.
Shen, J., Liu, J., Qin, L., Wang, S.J., Li, S., Xia, J., Ke, S. and Yang, J. (2015) Chromium isotope signature during continental crust subduction recorded in metamorphic rocks. *Geochem. Geophys. Geosyst.* **16**, 3840-3854.

Shen, J., Qin, L., Fang, Z., Zhang, Y., Liu, J., Liu, W., Wang, F., Xiao, Y., Yu, H. and Wei, S. (2018) High-temperature inter-mineral Cr isotope fractionation: A comparison of ionic model predictions and experimental investigations of mantle xenoliths from the North China Craton. *Earth Planet. Sci. Lett.* **499**, 278-290.

Siebert, J., Badro, J., Antonangeli, D. and Ryerson, F.J. (2013) Terrestrial Accretion Under Oxidizing Conditions. *Science* **339**, 1194-1197.

Siebert, J., Sossi, P.A., Blanchard, I., Mahan, B., Badro, J. and Moynier, F. (2018) Chondritic Mn/Na ratio and limited post-nebular volatile loss of the Earth. *Earth Planet. Sci. Lett.* **485**, 130-139.

Sossi, P.A., Moynier, F. and van Zuilen, K. (2018) Volatile loss following cooling and accretion of the Moon revealed by chromium isotopes. *Proc. Natl. Acad. Sci.* doi/10.1073/pnas.1809060115

Sossi, P. A., and Fegley Jr, B. (2018). Thermodynamics of element volatility and its application to planetary processes. *Reviews in Mineralogy and Geochemistry*, **84**, 393-459.

Sossi P.A., Klemme S., O'Neill H. St.C., Berndt J. and Moynier F. (2019). Evaporation of moderately volatile elements from silicate melts: experiments and theory. Geochim. Cosmochim. Acta. In press. doi: 10.1016/j.gca.2019.06.021

Stolper, E. (1977) Experimental petrology of eucritic meteorites. *Geochim. Cosmochim. Acta* **41**, 587-611.

Tian, Z., Chen, H., Fegley, B.J., Lodders, K., Barrat, J.A. and Wang, K. (2018) Potassium Isotope Differences Among Chondrites, Earth, Moon, Mars, and 4-Vesta — Implication on the Planet Accretion Mechanisms, *49th Lunar Planet. Sci. Conf. Texas.* #2083 (abstr.)

Toplis, M. J. (2005). The thermodynamics of iron and magnesium partitioning between olivine and liquid: criteria for assessing and predicting equilibrium in natural and experimental systems. *Contributions to Mineralogy and Petrology*. **149**, 22-39.

Trinquier, A., Birck, J.-L. and Allègre, C.J. (2007) Widespread ^{54}Cr heterogeneity in the inner solar system. *Astrophys. J.* **655**, 1179.

Trinquier, A., Birck, J.L., Allègre, C.J., Göpel, C. and Ulfbeck, D. (2008) ^{53}Mn–^{53}Cr systematics of the early Solar System revisited. *Geochim. Cosmochim. Acta* **72**, 5146-5163.

Trinquier, A., Elliott, T., Ulfbeck, D., Coath, C., Krot, A. N., and Bizzarro, M. (2009). Origin of nucleosynthetic isotope heterogeneity in the solar protoplanetary disk. *Science* **324**, 374-376.

Visscher, C. and Fegley Jr, B. (2013) Chemistry of impact-generated silicate melt-vapor debris disks. *Astrophys. J. Lett.* **767**, L12.

Wadhwa, M. (2008) Redox conditions on small bodies, the Moon and Mars. *Reviews in Mineralogy and Geochemistry* **68**, 493-510.

Wade, J., & Wood, B. J. (2001). The Earth's 'missing'niobium may be in the core. *Nature* **409**, 75-78.

Wang, K. and Jacobsen, S.B. (2016) Potassium isotopic evidence for a high-energy giant impact origin of the Moon. *Nature* **538**, 487-490.

Wänke, H. and Dreibus, G. (1980) The bulk composition of the eucrite parent asteroid and its bearing on planetary evolution. *Zeitschrift für Naturforschung A* **35**, 204-216.

Warren, P.H., Kallemeyn, G.W., Huber, H., Ulff-Møller, F. and Choe, W. (2009) Siderophile and other geochemical constraints on mixing relationships among HED-meteoritic breccias. *Geochim. Cosmochim. Acta* **73**, 5918-5943.

907 Wasson, J.T. and Kallemeyn, G.W. (1988) Compositions of chondrites. *Phil. Trans. R. Soc. A.*
908 **325**, 535-544.
909 Wilson, L. and Keil, K. (2017) Arguments for the non-existence of magma oceans in asteroids.
910 In Planetesimals: Early Differentiation and Consequences for Planets. Cambridge University
911 Press, Cambridge Planetary Science, 159-179.
912 Wood, B.J., Wade, J. and Kilburn, M.R. (2008) Core formation and the oxidation state of the
913 Earth: Additional constraints from Nb, V and Cr partitioning. *Geochim. Cosmochim. Acta* **72**,
914 1415-1426.
915 Xia, J., Qin, L., Shen, J., Carlson, R.W., Ionov, D.A. and Mock, T.D. (2017) Chromium isotope
916 heterogeneity in the mantle. *Earth Planet. Sci. Lett.* **464**, 103-115.
917 Young, E. D., Shahar, A., Nimmo, F., Schlichting, H. E., Schauble, E. A., Tang, H. and Labidi, J.
918 (2019). Near-equilibrium isotope fractionation during planetesimal evaporation. *Icarus*. **323**, 1-
919 15
920 Zhu, K., Liu, J., Moynier, F., Qin, L., Alexander, C. M. D., and He, Y. (2019a). Chromium Isotopic
921 Evidence for an Early Formation of Chondrules from the Ornans CO Chondrite. *Astrophys.*
922 *J.*, **873**, 82.
923 Zhu, K., Moynier, F., Barrat, J.-A., Wielandt, D., Larsen, K. and Bizzarro, M. (2019b). Timing
924 and origin of the angrite parent body inferred from Cr isotopes. *Astrophys. J. Lett.*, **877**, L13

925